Journal of General Virology (2011), **92**, 572–581 **DOI** 10.1099/vir.0.027714-0

Hepatitis E virus replication involves alternating negative- and positive-sense RNA synthesis

Satya Pavan Kumar Varma,[1] Amit Kumar,[1] Neeraj Kapur,[1] Hemlata Durgapal,[1] Subrat Kumar Acharya[2] and Subrat Kumar Panda[1]

Correspondence
Subrat Kumar Panda
subrat@gmail.com

[1]Department of Pathology, All India Institute of Medical Sciences, Ansari Nagar, New Delhi 110029, India

[2]Department of Gastroenterology, All India Institute of Medical Sciences, Ansari Nagar, New Delhi 110029, India

Hepatitis E virus (HEV) is the major cause of epidemic hepatitis and many outbreaks of sporadic hepatitis. The virus responsible has a single-stranded, positive-sense RNA. Its replication and the regulatory process involved therein are poorly understood. Much of the HEV biology studied has been done by using full-length capped RNA transcripts (replicons) and transient transfections in cell cultures. We investigated replicon replication using negative-sense strand-specific molecular beacons in live cell imaging, and quantifying intracellular viral RNA using strand-specific real-time PCR every 2 h until 24 h post-transfection. A graph of the copy numbers of both positive- and negative-sense RNA at the different time points was plotted. This showed a temporal separation and alternating cycles of negative- and positive-sense RNA formation. As a control, a dysfunctional replicase mutant (GDD→GAA) was used, which showed no increase in copy number. The live cell imaging corroborated the quantitative data, in that the maximal amount of negative-sense RNA was observed at 8 h post-transfection. The real-time-PCR copy-number analysis of the subgenome showed the presence of a single subgenomic RNA. Using fluorescent protein genes *mCherry* and *EGFP* fused in-frame to *ORF2* and *ORF3* in separate constructs and immunofluorescence, we showed the formation of both proteins pORF2 and pORF3 from a single subgenomic RNA. Our study demonstrated cyclical bursts of virus replication and the role of subgenomic RNA in the HEV life cycle.

Received 1 October 2010
Accepted 29 November 2010

INTRODUCTION

Hepatitis E virus (HEV) is an enterically transmitted agent of acute viral hepatitis (Vishwanathan, 1957; Wong *et al.*, 1980; Balayan *et al.*, 1983). It is a 27–34 nm non-enveloped virion that has a single-stranded positive-sense, capped and polyadenylated RNA of approximately 7.2 kb in length (Reyes *et al.*, 1990, 1993; Tam *et al.*, 1991; Aye *et al.*, 1993; Purdy *et al.*, 1993; Nanda *et al.*, 1994; Kabrane-Lazizi *et al.*, 1999). HEV was placed in a separate genus, *Hepevirus*. With four recognized genotypes it is a major cause of sporadic as well as epidemic hepatitis globally (Emerson *et al.*, 2004a).

The genome is organized into three ORFs. The 27–35 nt long 5′ non-coding region (NCR) is followed by *ORF1*, which encodes the non-structural polyprotein (Ansari *et al.*, 2000). Computer-assisted analyses of HEV *ORF1* suggested the presence of methyltransferase-, putative cysteine-protease-, RNA helicase- and RNA-dependent RNA polymerase (*RdRp*)-homology domains (Koonin *et al.*, 1992). The functional activities of pRdRp (Agrawal *et al.*, 2001), helicase (Karpe & Lole, 2010) and methyltransferase (Magden *et al.*, 2001) have been verified experimentally. *ORF2* encodes the major viral capsid protein (pORF2), which contains a signal peptide and potential glycosylation, dimerization and host interacting sites (Jameel *et al.*, 1996; Li *et al.*, 2009; Guu *et al.*, 2009; Yamashita *et al.*, 2009). It has been found that *ORF3* overlaps with *ORF2*, encodes a small 114 aa protein and that both pORF3 and pORF2 are formed from a single subgenomic RNA (Graff *et al.*, 2006; Huang *et al.*, 2007). No discrete function has been assigned to pORF3 except that it is a cytoskeleton-associated protein that may be involved in host interactions, virion assembly and exit (Zafrullah *et al.*, 1997; Moin *et al.*, 2007, 2009; Chandra *et al.*, 2008; Takahashi *et al.*, 2008; Kannan *et al.*, 2009; Yamada *et al.*, 2009). The 3′ NCR is 65–74 nt long, contains *cis*-acting elements for pRdRp binding and ends in a poly(A) tail (Agrawal *et al.*, 2001).

Transient transfections of full-length capped RNA transcripts (replicons) in cell culture have helped to delineate

The GenBank/EMBL/DDBJ accession number for the sequence of a newly constructed full-length HEV clone derived from human bile is FJ457024.

A supplementary figure, two supplementary tables and a video are available with the online version of this paper.

the events during the HEV replication cycle (Panda *et al.*, 1995, 2000; Thakral *et al.*, 2005). It is essential to understand the replicon life cycle in such systems, especially as a function of time, so as to allow easy understanding of the stages of replication and the regulation involved. However, inherent technical problems in transient transfection systems made such studies difficult. In the recent past PLC/PRF/5 and A549 cells have been shown to be susceptible to HEV infection (Tanaka *et al.*, 2007). Several clinical studies carried out recently (Kumar Acharya *et al.*, 2007; Zhang *et al.*, 2006; Fan *et al.*, 2007) have demonstrated a poor prognosis when HEV superinfects chronic hepatitis B virus-infected individuals. The PLC/PRF/5 cell line, with several integrated hepatitis B virus (HBV) genes, may affect HEV replication in ways unknown to us, and A549 is a non-hepatic cell line. Therefore, the replicon-transfection method described by us remains the best method for studying HEV replication, even though it excludes the steps of attachment, entry and release of the genome. The use of antibiotic selection and stable cell lines helped in producing accumulative data, such as the possibility of a single subgenomic RNA of 2.2 kb (Graff *et al.*, 2006) and pRdRp localization (Rehman *et al.*, 2008). The above studies have helped in elucidating the different stages in HEV replication but none could provide a timescale analysis of the process.

In this report we have constructed a new full-length cDNA clone of a genotype 1 HEV that was isolated directly from a human patient without animal passage, studied the replication of the transfected replicon over a time and observed a cyclical process that was unknown to date.

RESULTS

Detection of full-length HEV replicon replication

Upon electroporation of Huh7 cells, the *in vitro*-generated capped polyadenylated RNA transcripts (replicons) from a newly constructed full-length HEV clone (genotype 1) (pSGHEV-HB, GenBank accession no. FJ457024; Supplementary Fig. S1, available in JGV Online) derived from human bile, collected post-mortem, demonstrated negative-sense RNA synthesis as well as expressing virally encoded proteins (Figs 1 and 2). Cells were co-transfected with HEV replicon and molecular beacons (Rehman *et al.*, 2008) specific for negative-sense viral RNA, and cells were scanned for beacon-induced fluorescence beginning from 4 h post-transfection. Faint signals were picked up at 5 h post-transfection (Fig. 1a) and, during time-lapse imaging, intensified up to 8 h (Fig. 1c), fading thereafter by 12 h (Fig. 1d) (Video as Supplementary Data, available in JGV Online). Mock-transfected cells and cells transfected with replicon containing dysfunctional replicase (pSGHEV-HBmutRdRp) and the beacon showed no fluorescence (Fig. 1e).

Indirect immunofluorescence assays, carried out at 72 h post-transfection to detect viral proteins from the replicon (pSGHEV-HB) with anti-ORF2- and anti-ORF3-specific rabbit polyclonal antibodies, demonstrated the presence of proteins (Fig. 2a, b). Cells transfected with mutant replicons (pSGHEV-HBmutRdRp) showed no fluorescence (Fig. 2e). Huh7 cells transfected with pcDNA3ORF2 and pcDNA3ORF3 served as positive controls (Fig. 2c, d).

Analysis of viral genomic, subgenomic and negative-sense RNA at different time points

Capped, polyadenylated replicons generated by *in vitro* transcription (IVT) used for transfection experiments to study the virus life cycle were DNase treated to remove any remnant plasmids. This was confirmed by using gel electrophoresis (Fig. 3a) and by strand-specific PCR (Fig. 3b) using primer 6880FP (Supplementary Table S2, available in JGV Online) during reverse transcription. This also confirmed the strand specificity of our experiment as described by us previously in Panda *et al.* (2000) and Rehman *et al.* (2008).

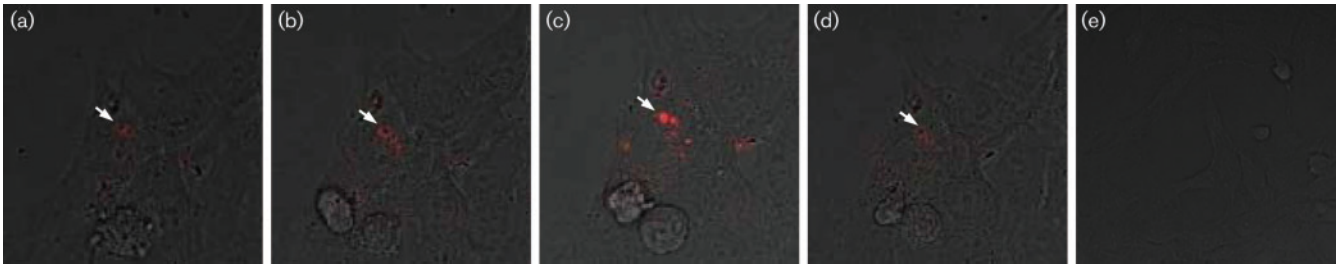

Fig. 1. Confocal live cell imaging for detection of negative-sense RNA from HEV (genotype 1) cDNA clone (pSGHEV-HB). Frames from confocal live cell imaging of Huh7 cells co-transfected with molecular beacon (BHQ2-6064-6083-Alexa 546) and *in vitro* transcribed capped polyadenylated replicons from pSGHEV-HB (a–d) or pSGHEV-HBmutRdRp (e). The molecular beacon is specific for negative-sense viral RNA replicative intermediate and the images in the figure show a gradual increase in fluorescent signal through time in panels (a–d): 5 h (a), 6 h (b), 8 h (c) and fading thereafter by 12 h (d) post-transfection. The arrows point to the fluorescence from the same cell at different time points. Cells transfected with replicons from pSGHEV-HBmutRdRp and beacons showed no fluorescence (e).

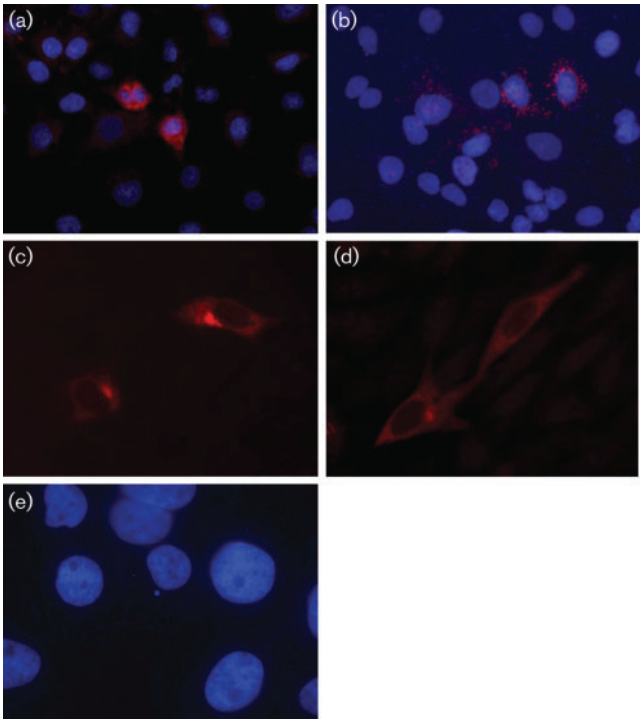

Fig. 2. Indirect Immunofluorescence microscopy for the detection of HEV pORF2 and pORF3 proteins from full-length HEV (genotype 1) cDNA clone (pSGHEV-HB GenBank accession no. FJ457024). Replicon-transfected Huh7 cells were stained for HEV pORF2 and HEV pORF3 at 72 h post-transfection using rabbit polyclonal antibodies specific for pORF2 and pORF3, respectively, followed by secondary antibody with Alexa 546-conjugated goat anti-rabbit antibodies in an indirect immunofluorescence assay. The nuclei were counterstained with DAPI. Cells transfected with replicons from pSGHEV-HB showed fluorescence corresponding to Alexa 546, confirming the formation of pORF2 (a) and pORF3 (b). Replication-defective dysfunctional mutant replicon pSGHEV-HBmutRdRP, used as a negative control, showed no fluorescence (e). Huh7 cells transfected with pcDNA3ORF2 and pcDNA3ORF3 served as positive controls (c, d).

Electroporation of replicons into a suspension of serum-starved (for 24 h) host cells (10^7 cells), and later distributing them into culture plates, allowed for uniformity of transfected cells in each plate and for approximate synchronization of the cell population. Electroporation resulted in 30–35 % cell death, as determined by monitoring the viable cell counts after electroporation and before plating. Plates were harvested every 2 h post-electroporation and the RNA isolated and quantified. Viral copy numbers obtained by real-time PCR quantification from 2 µg of input RNA were used to calculate the total number of virus copies present in the plate. The copy numbers were further normalised for variation in electroporation efficiency, and graphs (Fig. 4) were plotted with these values. The copy number versus time point plots for negative-sense RNA (Fig. 4b, c) showed an early burst with copy number reaching a maximum (1.2×10^6) at 8 h from 4×10^5 copies at

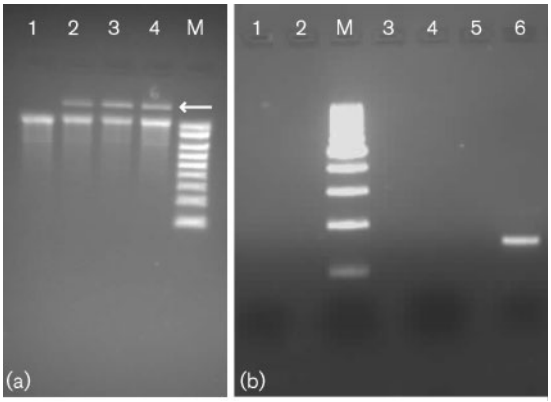

Fig. 3. Removal of the remnant plasmid from *in vitro*-transcribed replicons used in transfection experiments. Replicons used in transfections were made free of any plasmid DNA by DNase digestion. (a) A 1 % formaldehyde–agarose gel showing the *in vitro*-synthesized RNA of 7.2 kb. The DNase-digested product in the first lane shows the absence of any remnant plasmid. Arrow, Remnant plasmid. M, RNA millenium marker (Ambion). (b) Strand-specific PCR amplification of the remnant DNA from a non-digested IVT, which, as the digested products in lanes 1 and 4 are free of any amplicons, also shows the strand specificity of the primers and the specificity of the procedure. M, 700 bp DNA ladder (Fermentas).

4 h, followed by a constant copy number of approximately 5×10^5 from 12 to 24 h. Cells harvested immediately post-transfection showed no negative-sense RNA, while cells harvested at 2 h post-electroporation had ~5×10^2 copies (Fig. 4b, c; Supplementary Table S1, available in JGV Online). This matched up with our real-time live cell imaging, where the brightest beacon-induced fluorescence was seen at 8 h (Fig. 1c) (Supplementary Video). Negative-sense RNA was analysed using two primer pairs, one falling in the *ORF1* region (2589–2714) and the other in the *ORF2* region (6880–7038). Both the amplicons showed similar copy numbers (Fig. 4b, c, Supplementary Table S1). The cells transfected with the GDD mutant-defective replicon showed no negative-sense RNA (Fig. 4b, c).

The positive-sense genomic and subgenomic RNA of HEV were analysed using three primer pairs falling in the *ORF1*, *ORF2* and the earlier described 3.7 kb subgenomic region (Tam *et al.*, 1991; Xia *et al.*, 2000). The three amplicons used were: 2589–2714 (*ORF1*), 6880–7038 (*ORF2*) and 4554–4705 (3.7 kb hypothetical subgenomic RNA region). The 2589 amplicon was used to estimate genomic RNA. The 6880 amplicon in comparison with amplicons 2589 and 4554 was used for identification of the 2.2 kb subgenomic RNA. In addition, amplicon 4554 was used for analysing the existence of the 3.7 kb subgenome.

The positive-sense strands were present at 10^3-fold higher copy numbers than the negative-sense strands (Fig. 4; Supplementary Table S1). The copy number versus time plot for positive-sense RNA showed three peaks at 8, 14

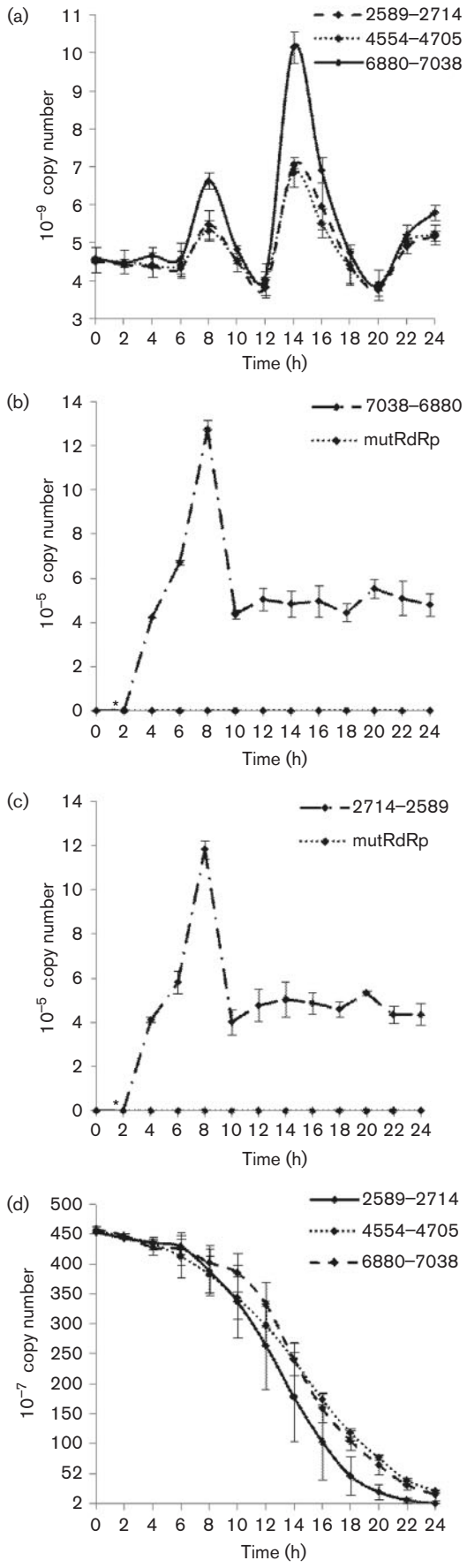

Fig. 4. Strand-specific real-time PCR analysis of the intracellular viral copy numbers up to 24 h post-electroporation. The graphs represent the strand-specific real-time PCR-quantified copy numbers for three different regions of the genome (both positive- and negative-sense) every 2 h post-transfection, for replicons pSGHEV-HB or pSGHEV-HBmutRdRp. The experiments were in triplicate and the plots developed with error bars, showing SD, with distinct patterns of copy numbers for the wild-type and mutant replicons. (a) Graph of the positive-sense RNA copy numbers from regions 2589, 4554 and 6880 obtained at different time points from pSGHEV-HB-replicon-electroporated cells showing cyclical bursts of positive sense RNA formation. (b, c) Graphs of negative-sense copy numbers from the 6880 and 2589 regions, respectively, at different time points, showing the greatest copy numbers at 8 h, unlike the positive-sense peak at 14 h, thus showing a temporal separation between them. *, Indicates the copy numbers of negative-sense RNA from pSGHEV-HB at 2 h post-transfection (~500 copies; Supplementary Table S1). These graphs (b, c) also show the copy numbers of the negative-sense strand from the 6880 and 2589 regions from the pSGHEV-HBmutRdRp replicon. (d) Graph of the positive-sense strand copy numbers from three regions, 2589, 4554 and 6880, obtained at different time points from pSGHEV-HBmutRdRP-replicon-electroporated cells showing a gradual decay of the copy number of the transfected replicon.

and 24 h. The positive-sense-strand copy numbers were highest at 14 h post-transfection. This was after the initial peak for the negative-sense strands at 8 h. At 14 h the 6880 amplicon had a copy number of 1.0×10^{10} as compared with 6.8×10^{9} copies of the 2589 and 4554 amplicons (Fig. 4a; Supplementary Table S1). There were comparable bursts in copy number for the positive-sense strands at 8 and 24 h, with the copy number of the 6880 amplicon being clearly higher than those of the 2589 and 4554 amplicons. The subgenomic RNA, as identified by amplicon 6880, was present in excess at 8, 14 and 24 h and at the rest of the time points was in concordance with the copy numbers of the genomic RNA. Both the 2589 and 4554 regions showed similar copy numbers and were always lesser than the copy number of the 6880 amplicon, especially at 8, 14 and 24 h, indicating the presence of smaller single subgenomic RNA. The predicted 3.7 kb subgenomic RNA was not confirmed. The GDD replicase mutant pSGHEV-HBmutRdRp showed no increase in copy numbers. On the other hand, the copy numbers declined over the time points taken (Fig. 4d; Supplementary Table S1), indicating decay in the transfected RNA.

Subgenomic RNA and structural protein expression

The ability of the single subgenomic RNA (Graff *et al.*, 2006; Huang *et al.*, 2007) to produce both pORF2 and pORF3 was tested using *in vitro*-synthesized capped subgenomic RNA SG-ORF2mCherry produced from construct pSGHEV-HB-ORF2mCherry and SG-ORF3EGFP produced from construct pSGHEV-HB-ORF3EGFP (Fig. 5).

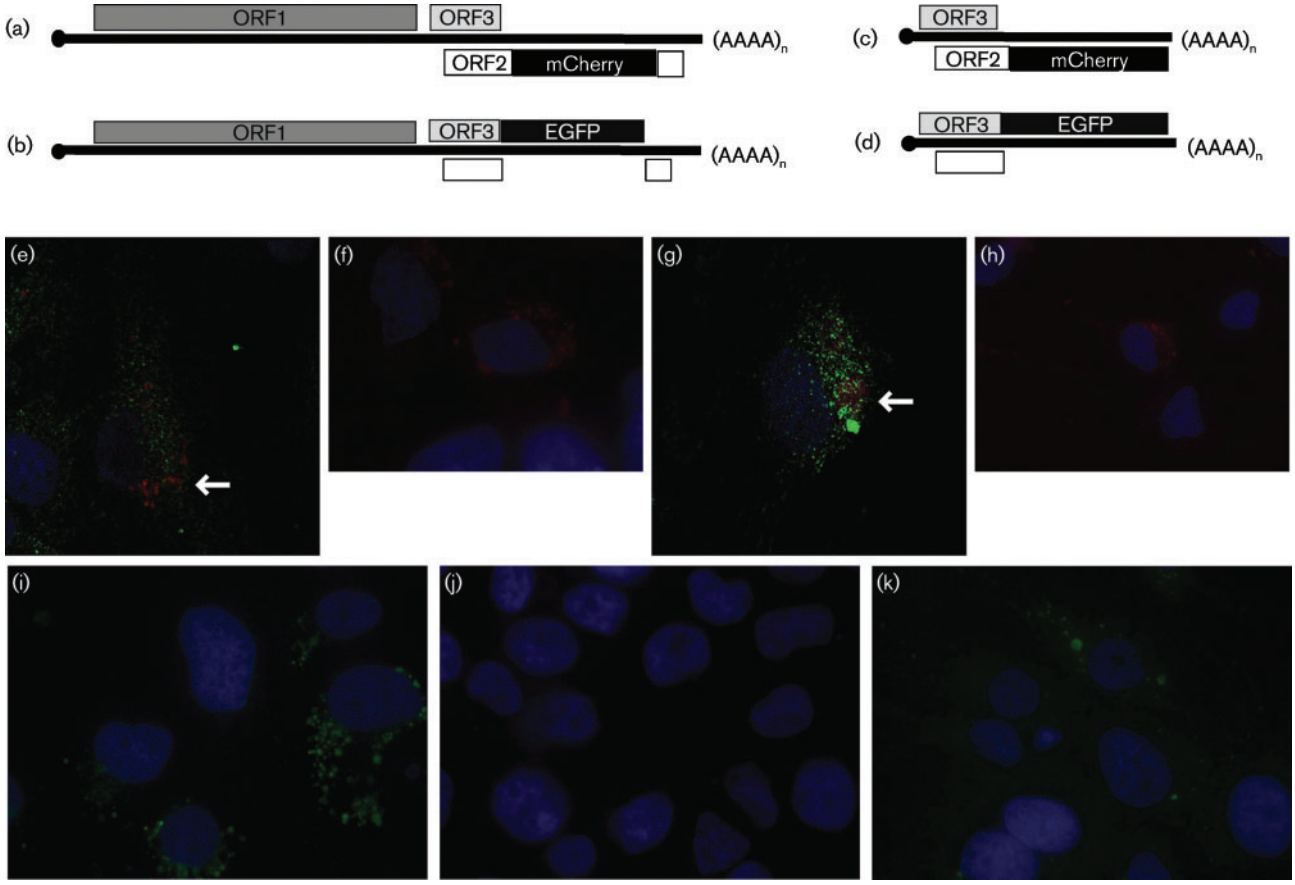

Fig. 5. Autofluorescence and indirect immunofluorescence imaging to detect the formation of both pORF2 and pORF3 from a single subgenomic RNA. Full-length fluorescent reporter-gene-fused cDNA constructs from a pSGHEV-HB clone were made with mCherry fused in-frame with ORF2 to form pSGHEV-HBORF2mCherry (a) and EGFP fused in-frame ORF3 to form pSGHEV-HBORF3EGFP (b). Cells were transfected with replicons from these full-length constructs and were fixed 72 h post-transfection. mCherry fluorescent signal indicating pORF2 formation (f) and EGFP fluorescent signal indicating pORF3 formation (i). Cells were transfected with *in vitro*-synthesized capped subgenomic RNA from the constructs shown in (c) and (d) and were fixed 24 h post-transfection. (h) Shows mCherry fluorescent signal indicating pORF2 formation and (k) shows EGFP fluorescent signal indicating pORF3 formation. Cells transfected with replicons from pSGHEV-HBORF2mCherry and SG-ORF2mCherry transcripts (a, c) were additionally subjected to an indirect immunofluorescent protocol to detect pORF3 production using mouse anti-pORF3 mAb (raised in house), and FITC-conjugated goat anti-mouse secondary antibody. Both full-length replicons and subgenomic transcripts from mCherry constructs displayed FITC fluorescence together with mCherry fluorescence showing formation of pORF3 and pORF2 (e, g). Mock transfected cells showed no auto or immunofluorescence (j). The arrows in panels (e) and (g) indicate mCherry fluorescence.

Cells electroporated with SG-ORF3EGFP or replicons from pSGHEV-HBORF3EGFP and fixed 24 and 72 h post-transfection showed EGFP autofluorescence indicating pORF3 formation (Fig. 5i, k). Similarly, cells electroporated with SG-ORF2mCherry showed cherry red autofluorescence (Fig. 5h) and additionally indirect immunofluorescence was performed for detecting pORF3 in SG-ORF2mCherry-transfected cells. Cells showed green FITC immunofluorescence signals from the same cells showing mCherry autofluorescence, corresponding to pORF3 and pORF2 expression (Fig. 5g). Similar autofluorescence and immunofluorescence signals were observed in the full-length replicon pSGHEV-HBORF2mCherry-transfected cells (Fig. 5e, f). This result confirms the earlier described single subgenomic RNA, the start site of the subgenomic RNA and the described AUG start codons for pORF3 and pORF2 (Graff *et al.*, 2006).

DISCUSSION

The virus replication cycle has only been studied in great detail in a handful of viruses. These are the ones that have a facile growth and cytopathic effect (Sawicki & Sawicki, 1980; Strauss & Strauss, 1994). In the absence of these two characteristics it is difficult to study the replication cycle of a virus in detail. For such viruses, transfecting cell lines

with replicons rescued from cDNA clones is an alternative strategy. The only *in vitro* cell-culture system developed for HEV in PLC/PRF/5 and A549 cell lines is not yet well characterized (Tanaka *et al.*, 2007). PLC/PRF/5 contains an integrated HBV genome, and the mutual interaction between the viruses (HBV and HEV) is yet to be defined. Therefore, study of the transient-transfection system over a time course is the best alternative method to understand HEV biology (Panda *et al.*, 2000).

Briefly, a cDNA clone (pSGHEV-HB) of HEV was constructed and the replication of its replicon in Huh7 cells was studied using strand-specific real-time PCR of intracellular viral RNA and by live cell imaging of the negative-sense strand using molecular beacons. A defective replicase mutant of the same clone (pSGHEV-HBmutRdRp) was used as a control. Cells were transfected by electroporation, which helped to produce uniform transfected cells in each culture plate. Approximate synchronization of cell cultures before transfection further helped in normalizing the variability, as seen by the total RNA yield from each plate (18-20 μg). In our earlier study the negative-sense strand of HEV was detected 6 h post-transfection (Thakral *et al.*, 2005). Hence we quantified viral RNA every 2 h until 24 h post-transfection.

The real-time RNA quantification showed a temporally separated increase in the positive-sense and negative-sense RNA (Fig. 4). Furthermore, negative-sense RNA intermediate was prominent only at the initial time points (up to 8 h) (Fig. 4b, c). Live cell beacon-induced fluorescent imaging for the negative-sense RNA showed its formation as early as 5 h post-transfection, peaked at 8 h post-transfection (Figure. 1a, c) and became faint by 12 h post-transfection and beyond. For the first time, we describe visualization of negative-sense RNA as it is formed, using live cell imaging (Fig. 1), and this corroborated the data obtained from real-time PCR.

The low negative-sense RNA copy number (~500 copies) at 2 h is explained by the time taken for cell stabilization after electroporation and for replicase generation. The burst in copy number at 4 h post-transfection and its rapid increase until 8 h post-transfection is due to newly synthesized replicase and the presence of larger amounts of input RNA (Fig. 4; Supplementary Table S1). Beyond this point the copy number of the antisense RNA reduced to $\sim 10^5$ copies, for the 24 h during which we tested, similar to what was observed for other viruses (Sawicki & Sawicki, 1980; Strauss & Strauss, 1994). There must be similar subtle regulatory mechanisms in play which are yet to be understood in HEV. Further negative-sense RNA copy numbers analysed using two amplicons, which fall in the subgenomic region (nt 6880–7038) and *ORF1* region (nt 2714–2589), had similar copy numbers (Fig. 4b, c), nullifying the possibility of any negative-sense subgenomic RNA.

The positive-sense RNA increased with time; peak copy number was detected at 14 h, 6 h after the negative-sense RNA. This alternate pattern of negative- and positive-sense RNA formation serves as an important host-defence evasion mechanism (Sawicki & Sawicki, 1980; Strauss & Strauss, 1994). Studies involving quantification of positive- and negative-sense RNA over a time frame in alphaviruses (Semliki Forest virus and Sindbis virus) have shown a temporal separation and alternate increase of positive and negative strands. No such studies are available for non-culturable and non-cytopathic viruses like HEV.

The existence of the two 3′-co-terminal subgenomic RNA (Tam *et al.*, 1991; Xia *et al.*, 2000) has remained intriguing. Recent reports show a single 2.2 kb subgenomic RNA by using probes falling only in the 3′ end of the genome (Graff *et al.*, 2006); they also speculated that the earlier 3.7 kb fragment might be a defective virus. Our analysis, involving both regions (4554 and 6880 amplicons), favours the single 3′-terminal subgenomic RNA, as described by Graff *et al.* (2006). The 6880 amplicon, during the positive-sense peak at 14 h, showed a higher copy number (1.0×10^{10}) than the 2589 and 4554 amplicons (6.8×10^9), which were identical in number (Supplementary Table S1). Thus we can infer that there are additional RNA species in the form of subgenomic RNA in the described region (Fig. 4). The 2589 and 4554 amplicon copy numbers were similar throughout the time course; no existence of the earlier predicted 3.7 kb subgenomic RNA was indicated (Tam *et al.*, 1991; Xia *et al.*, 2000). The replicase-mutant control showed no increase in copy number over the entire time period of the study (Fig. 4d), showing the importance of the GDD catalytic domain in the overall activity of the replicase (Emerson *et al.*, 2004b). This comparison paves the way to similar studies for understanding the involvement of other non-structural proteins in HEV replication.

The positive-sense strand peaks at 8, 14 and 24 h showed high copy numbers for subgenomic RNA (Fig. 4a), which indicates the importance and necessity of structural protein, before the availability of genomic RNA, for packaging. We presume that a virus-infected cell behaves like a factory where raw materials and components for assembly are produced before the final product (a burst of virus release), and the process is repeated again, especially in a non-cytopathic virus like HEV.

Considering the potential of the single subgenomic RNA in the HEV life cycle, we tried to confirm its ability to translate the proteins pORF2 and pORF3, by using fluorescent proteins placed in-frame. *In vitro*-synthesized capped subgenomic RNA made to form from the earlier described start site, nt 5122 (Graff *et al.*, 2006) (nt 5124 in case of the FJ457024 clone) were transfected and were shown to form pORF2 and pORF3. An alternative indirect immunofluorescence experiment showed the production of both proteins, pORF2 and pORF3 (Fig. 5g). This is the first time any such visual confirmation of the formation of pORF2 and pORF3 from the single subgenomic RNA has been obtained.

The complexity shown in the replication of HEV is possible only by a subtle regulation process involving the processing of viral non-structural proteins and regulation of cellular

protein machinery (Sawicki & Sawicki, 1980). HEV pORF1 is processed only in the context of replication (Ansari *et al.*, 2000). Sehgal *et al.* (2006) showed abnormal pORF1 processing in a baculovirus system. The speculation that pORF1 processing might have a role in the regulation of replication could be interesting.

Our study demonstrated a cyclical pattern of virus growth in the case of acutely infecting non-cytopathic HEV, which has not been described before. We also reconfirm the presence of a single subgenomic RNA expressing two of the viral proteins (pORF2 and pORF3).

METHODS

Assembly of a full-length cDNA clone of HEV (genotype 1), isolated from human bile (pSGHEV-HB). We constructed a full-length cDNA clone (pSGHEV-HB, GenBank accession no: FJ457024) of a HEV isolate (genotype 1) from bile, collected post-mortem with the necessary consent, from a patient who had acute liver failure. RNA was isolated from 100 µl of bile sample using a TRIzol method (Invitrogen) as per the manufacturer's instructions and was subjected to reverse transcription with primers designed using a previously published HEV genome (AF076239) from India (Supplementary Table S2). The HEV genome was amplified in five overlapping contiguous portions (nt 1–1225nt, nt 1203–2966, nt 2544–4873, nt 4413–5815 and nt 5601–7194) and cloned into pPCR-Script Amp SK(+) (Stratagene) using a PCR-Script Amp cloning kit as per the manufacturer's instructions. 5′ and 3′ RACE for the extreme ends were performed and the sequences cross checked with nt 1-1208 and nt 5601-7194. The latter was replaced with the 3′-end RACE product. The above clones were used for reconstruction of the full-length cDNA clone (Supplementary Fig. S1). All clones mentioned above and hereafter were confirmed by sequencing by using Big Dye Terminator 3.0 (Applied Biosystems) in an ABI 310 automated sequencer (Perkin Elmer).

Construction of an RdRp functional mutant (pSGHEV-HBmut*RdRp*). A functional mutant of *RdRp* was generated by mutating the GDD catalytic triad to GAA in a pSGHEV-HB clone using a primer pair containing the altered sequence (Supplementary Table S2) to introduce the mutation using a Sure-Site mutagenesis kit (Stratagene) as per the manufacturer's instructions.

Construction of fluorescent reporter replicons. The replicon pSGHEV-HB-ORF2mCherry was constructed by replacing nt 5488–6964 of pSGHEV-HB with an mCherry gene. The remaining partial fragment of HEV ORF2 was then out of frame (Fig. 5a). The mCherry gene was amplified by PCR from the plasmid pRSET-mCherry [kindly provided by Dr Roger Tsein, a Howard Hughes Medical Institute (HHMI) investigator, University of California San Diego, USA] by using a GFP FP and GFP RP primer pair (Supplementary Table S2) including the 3′ terminal *Nhe*I site. The 5′ end of the mCherry gene was extended with nt 4858–5488 of pSGHEV-HB, which was generated by fusion PCR using 4873 *Apa*I FP and ORF2 cherry RP primer pairs which included a 5′ terminal *Apa*I site (Supplementary Table S2). The resulting fused PCR product was digested with *Apa*I and *Nhe*I and substituted into pSGHEV-HB to yield pSGHEV-HB-ORF2-mCherry (Fig. 5a).

The construct pSGHEV-HB-ORF3-EGFP (Fig. 5b), in which the *EGFP* gene, placed in-frame with *ORF3*, was constructed by replacing nt 5475–6964 of pSGHEV-HB with an *EGFP* gene using a similar strategy.

***In vitro* production of capped full-length replicons and capped subgenomic transcripts.** pSGHEV-HB, pSGHEV-HBmutRdRp, pSGHEV-HB-ORF2mCherry and pSGHEV-HB-ORF3EGFP were digested with *Xho*I to produce DNA templates for run-off transcription. Linearized plasmids were *in vitro* transcribed to produce capped, full-length transcripts by using mMESSAGE mMACHINE T7 Ultra kits (Ambion, USA) as per the manufacturer's instructions. An additional 2 µl of the GTP provided was added to the reaction in view of the long transcripts. The reaction was incubated for 3 h at 37 °C and an additional 2 µl of T7 enzyme mix was added after 1.5 h. At the end of the incubation the input DNA was removed by DNase digestion and the reaction cleaned using phenol/chloroform extraction. The removal of remnant plasmid was checked both on a formaldehyde–agarose gel (Fig. 3a) and by strand-specific PCR (Rehman *et al.*, 2008) using the 6880FP and 6880RP primer pair (158 bp) (Fig. 3b; Supplementary Table S2,). *In vitro*-transcribed RNA was quantified using a Nanodrop spectrophotometer (Thermo Scientific).

Subgenomic transcripts were produced using a T7 promoter attached to a PCR product produced by amplifying nt 5124–6964 using primer pairs with an additional 5′ T7 promoter sequence (Supplementary Table S2). These amplicons from pSGHEV-HB-ORF2mCherry and pSGHEV-HB-ORF3EGFP were used to produce capped subgenomic transcripts SG-ORF2mCherry (Fig. 5c) and SG-ORF3EGFP (Fig. 5d), respectively, using an mMessage mMachine T7 ultra kit (Ambion) as per the manufacturer's instructions. Poly(A) tails were added to subgenomic transcripts by using poly(A) polymerase provided in an mMessage mMachine T7 ultra kit (Ambion) and used as per the manufacturer's instructions.

Cell culture and transfections. Huh7 cells (Human hepatoma cell line) were maintained in Dulbecco's modified Eagle's medium (DMEM) (Invitrogen) supplemented with 10 % heat-inactivated FBS (Invitrogen), and 1× antibiotic–antimycotic (100 µg ml^{-1} streptomycin and 100 U ml^{-1} penicillin; Sigma-Aldrich). Cells were subjected to serum starvation for 24 h prior to transfection by maintaining cells in DMEM supplemented with 2 % heat-inactivated FBS for 24 h and then releasing them by replenishing the culture with normal medium before transfection. Cells were maintained in an atmosphere of 5 % CO_2 at 37 °C before and after transfection.

Electroporation of Huh7 cells with HEV replicons. Confluent monolayers of Huh7 cells maintained in 125 cm^3 culture flasks (Corning) were trypsinized, and cell suspensions were made. Cell counting was done using a Neubauer chamber (Marienfeld). Cells (2×10^7) were taken and processed in two batches of 1×10^7 cells. The cells were pelleted and washed twice with transfection medium (serum-free 1× DMEM made in nuclease-free water). The cells were finally suspended in 0.5 ml transfection medium and 10 µg of the *in vitro*-transcribed RNA from pSGHEV-HB (~10 µl) was added to one batch and 10 µg of the *in vitro*-transcribed RNA from pSGHEV-HBmutRdRp was added to another batch. The two suspensions were then taken in two separate Gene Pulser electroporation cuvettes (0.4 cm electrode; Bio-Rad), and incubated at 4 °C for 5 min, followed by a brief pulse at 200 V, 975 µF in an electroporator (Gene Pulser II; Bio-Rad). After the pulse, cells in each cuvette were resuspended in complete medium and diluted up to 6 ml separately. Viable-cell counts were taken at this stage using trypan blue on a Neubauer chamber. The two suspensions were then equally distributed into two separate batches of 35 mm Petri plates such that 500 µl of the suspension was added to each plate (~$0.6–0.7 \times 10^6$ cells). The cells in each plate were layered with 2 ml media. The plates were incubated as described above.

Fluorescent replicons from pSGHEV-HB-ORF2-mCherry and pSGHEV-HB-ORF3-EGFP, and fluorescent subgenomic transcripts SG-ORF2-*mCherry* and SG-ORF3-*EGFP* were also electroporated as described above. However, the electroporated cell suspensions were plated on coverslips placed in 30 mm Petri dishes.

Replicons from pSGHEV-HB and mutant replicons from pSGHEV-HBmutRdRp for live cell imaging were electroporated as described above along with 100 nM of molecular beacon (BHQ2-6064-6083-Alexa 546; Operon Biotechnologies). The beacon designed was specific against negative-sense replicative intermediate (Rehman *et al.*, 2008). The cell suspensions were plated on LabTek II chambered cover glass (Nalge Nunc).

Two-step strand-specific real-time-PCR quantification of intracellular viral RNA.

Reverse transcription (step one). Every 2 h post-transfection one plate from each batch, i.e. one plate of pSGHEV-*HB* and one of pSGHEV-HBmutRdRp, was harvested. The supernatant was collected and any unattached cells present were pelleted, resuspended and put back into the tube so that no cell loss occurred. The pellets were washed in PBS (pH 7.4) and lysed in 1 ml TRIzol reagent. Total RNA was isolated and quantified spectrophotometrically. RNA from each plate was subjected to strand-specific reverse transcription (Rehman *et al.*, 2008) using five primers [2714 RP, 4705 RP, 7038 RP (for the positive-sense strand) and 6880 FP and 2589 FP (for the negative-sense strand); 300 nM each] in five separate reactions. The strand specificity of these primers and the process described above was tested using IVT product with a large amount of RNA used as a control in an experiment to detect negative-sense RNA, which showed no signal (Fig. 3b). Reverse transcription was carried out by using 2 μg total cellular RNA with 50 U Superscript RT-III enzyme (Invitrogen) in a 20 μl reaction at 55 °C for 1 h. Standards for absolute quantification in real-time PCR were made using serially diluted known quantities of transcripts from the pSGHEV-HB clone and were reverse transcribed using primer 7038 RP.

Real-time PCR (step two). Following cDNA synthesis, the RNA was degraded by digestion with 2.5 U RNase H (Ambion) and 0.75 μg RNase A (Ambion) at 37 °C for 30 min. Five microlitres of the reverse-transcribed product was used in a 50 μl cDNA amplification reaction with 300 nM forward and reverse primers (Supplementary Table S2) using SYBR Green PCR Core reagents (1.25 U AmpliTaq Gold, 0.5 U AmpErase; PE Biosystems). The reactions were set up in MicroAmp Optical 96-well reaction plates (Perkin Elmer Applied Biosystems), sealed and run on a Perkin Elmer ABI Prism 7700 Sequence Detection system (Applied Biosystems) with 40 cycles of annealing and extension (60 °C for 1 min) and denaturation (95 °C for 1 min).

The copy numbers from each plate were determined using the copy numbers obtained from 2 μg of total RNA, and a graph was plotted with copy number on the *y*-axis and time points on the *x*-axis. Furthermore, the copy numbers obtained for the normal and mutant replicons in all the repetitions were normalised using the post-electroporation viable cell counts. The reproducibility of electroporation and the real-time assay were checked by carrying out these assays in triplicate for both the wild-type and mutant replicons. The graphs were plotted with the mean copy numbers obtained from the three studies, with error bars showing SD.

Confocal live cell time-lapse imaging for monitoring negative-sense RNA replicative intermediate by the use of strand-specific molecular beacons. Huh7 cells were plated in LabTek II chambered cover glass (Nalge Nunc). Cells were monitored up to 12 h post-transfection after media change with a LEICA TCS SP5 confocal system with attached ludwin CO_2 incubator chamber and temperature control stage. For Alexa 546 excitation, He–Ne LASER lines were used. The scanning was done sequentially over a period of 8 h (4–12 h post-transfection) as a time lapse sequence with 10 min interval.

Fluorescent imaging and indirect immunofluorescence. Indirect Immunofluorescence was performed to detect expression of viral proteins (pORF2 and pORF3) in electroporated cells with a replicon from pSGHEV-HB and mutant replicons from pSGHEV-HBmutRdRp at 72 h post electroporation. Indirect immunofluorescence was also performed to detect pORF3 in cells electroporated with pSGHEV-HB-ORF2mCherry at 72 h post-electroporation and in cells electroporated with SG-ORF2mCherry at 24 h post-electroporation. Cells on the coverslips were washed three times with 0.05 M PBS (PBS pH 7.4, 137 mM NaCl, 2.7 mM KCl, 0.9 mM KH_2PO_4, 0.63 mM Na_2HPO_4), followed by fixing with 4 % paraformaldehyde (in 0.05 M PBS) at room temperature for 7 min. The cells were then washed with PBST (0.1 % Tween 20 in 1 × 0.05 M PBS), followed by permeabilization with 100 % methanol at −20 °C for 3 min. The cells were rehydrated with 0.05 M PBS for 20 min at room temperature. Blocking was carried out with 1 % BSA (Sigma) in 0.05 M PBS for 1 h at room temperature, followed by further blocking with 5 % normal goat serum (NGS) in PBST for 2 h at room temperature. Cells were then washed with PBST. After blocking, cells were incubated with primary antibody (rabbit anti-ORF2 and anti-ORF3; mouse anti-ORF3 monoclonal antibody for ORF2mCherry constructs) at 1 : 150 dilution prepared in blocking solution (1 % NGS in PBST) for 1 h at room temperature. The cells were then washed three times with PBST (10 min each wash). The primary-antibody labelled cells were further incubated with secondary antibody (goat anti-rabbit immunoglobulins conjugated with Alexa 546, goat anti-mouse immunoglobulins conjugated with FITC) in a 1 : 1000 dilution prepared in blocking solution (1 % NGS in PBST) for 30 min at room temperature. The cells were washed three times with PBST (10 min each wash) and mounted in 65 % glycerol prepared in PBS. Fluorescence was observed under a Nikon inverted fluorescence microscope (Eclipse TE 2000U) by excitation/emission at 556/573 nm and photographed.

Cells transfected with replicons from pSGHEV-HB-ORF3EGFP and SG-ORF3EGFP transcripts were fixed as described above and mounted directly for autofluorescent imaging.

ACKNOWLEDGEMENTS

This work was supported by a Grant-in-Aid from the Department of Biotechnology, Government of India, to Professor Subrat Kumar Panda, also a recipient of a J. C. Bose fellowship from the Department of Science and Technology, Government of India. Satya Pavan Kumar Varma is a recipient of a fellowship from the University Grants Commission, Government of India. Amit Kumar and Neeraj Kapur are recipients of fellowships from the Council of Scientific and Industrial Research, Government of India. mCherry used for the study was kindly provided by Dr Roger Tsein, an HHMI investigator, University of California San Diego, USA.

REFERENCES

Agrawal, S., Gupta, D. & Panda, S. K. (2001). The 3′ end of hepatitis E virus (HEV) genome binds specifically to the viral RNA-dependent RNA polymerase (RdRp). *Virology* **282**, 87–101.

Ansari, I. H., Nanda, S. K., Durgapal, H., Agrawal, S., Mohanty, S. K., Gupta, D., Jameel, S. & Panda, S. K. (2000). Cloning, sequencing, and expression of the hepatitis E virus (HEV) nonstructural open reading frame 1 (ORF1). *J Med Virol* **60**, 275–283.

Aye, T. T., Uchida, T., Ma, X., Iida, F., Shikata, T., Ichikawa, M., Rikihisa, T. & Win, K. M. (1993). Sequence and gene structure of the hepatitis E virus isolated from Myanmar. *Virus Genes* **7**, 95–109.

Balayan, M. S., Andjaparidze, A. G., Savinskaya, S. S., Ketiladze, E. S., Braginsky, D. M., Savinov, A. P. & Poleschuk, V. F. (1983).

Evidence for a virus in non-A, non-B hepatitis transmitted via the fecal-oral route. *Intervirology* **20**, 23–31.

Chandra, V., Kar-Roy, A., Kumari, S., Mayor, S. & Jameel, S. (2008). The hepatitis E virus ORF3 protein modulates epidermal growth factor receptor trafficking, STAT3 translocation, and the acute-phase response. *J Virol* **82**, 7100–7110.

Emerson, S. U., Anderson, D., Arankalle, A., Meng, X. J., Purdy, M., Schlauder, G. G. & Tsarev, S. A. (2004a.). Hepevirus. In *Virus Taxonomy: Eighth Report of the International Committee on Taxonomy of Viruses*, pp. 853–855. Edited by C. M. Fauquet, M. A. Mayo, J. Maniloff, U. Desselberger & L. A. Ball. London: Elesevier/Academic Press.

Emerson, S. U., Nguyen, H., Graff, J., Stephany, D. A., Brockington, A. & Purcell, R. H. (2004b). In vitro replication of hepatitis E virus (HEV) genomes and of an HEV replicon expressing green fluorescent protein. *J Virol* **78**, 4838–4846.

Fan, Z. P., Lin, S. H., Cai, S. P., Ji, Y. J., Gao, F., Zhang, H. Y., Luo, S. Q. & Zhang, W. J. (2007). An analysis of the clinical characteristics of patients with chronic hepatitis B superinfected with acute hepatitis E. *Zhonghua Shi Yan He Lin Chuang Bing Du Xue Za Zhi* **21**, 325–327 (in Chinese).

Graff, J., Torian, U., Nguyen, H. & Emerson, S. U. (2006). A bicistronic subgenomic mRNA encodes both the ORF2 and ORF3 proteins of hepatitis E virus. *J Virol* **80**, 5919–5926.

Guu, T. S., Liu, Z., Ye, Q., Mata, D. A., Li, K., Yin, C., Zhang, J. & Tao, Y. J. (2009). Structure of the hepatitis E virus-like particle suggests mechanisms for virus assembly and receptor binding. *Proc Natl Acad Sci U S A* **106**, 12992–12997.

Huang, Y. W., Opriessnig, T., Halbur, P. G. & Meng, X. J. (2007). Initiation at the third in-frame AUG codon of open reading frame 3 of the hepatitis E virus is essential for viral infectivity in vivo. *J Virol* **81**, 3018–3026.

Jameel, S., Zafrullah, M., Ozdener, M. H. & Panda, S. K. (1996). Expression in animal cells and characterization of the hepatitis E virus structural proteins. *J Virol* **70**, 207–216.

Kabrane-Lazizi, Y., Meng, X. J., Purcell, R. H. & Emerson, S. U. (1999). Evidence that the genomic RNA of hepatitis E virus is capped. *J Virol* **73**, 8848–8850.

Kannan, H., Fan, S., Patel, D., Bossis, I. & Zhang, Y. J. (2009). The hepatitis E virus open reading frame 3 product interacts with microtubules and interferes with their dynamics. *J Virol* **83**, 6375–6382.

Karpe, Y. A. & Lole, K. S. (2010). NTPase and 5′ to 3′ RNA duplex-unwinding activities of the hepatitis E virus helicase domain. *J Virol* **84**, 3595–3602.

Koonin, E. V., Gorbalenya, A. E., Purdy, M. A., Rozanov, M. N., Reyes, G. R. & Bradley, D. W. (1992). Computer-assisted assignment of functional domains in the nonstructural polyprotein of hepatitis E virus: delineation of an additional group of positive-strand RNA plant and animal viruses. *Proc Natl Acad Sci U S A* **89**, 8259–8263.

Kumar Acharya, S., Kumar Sharma, P., Singh, R., Kumar Mohanty, S., Madan, K., Kumar Jha, J. & Kumar Panda, S. (2007). Hepatitis E virus (HEV) infection in patients with cirrhosis is associated with rapid decompensation and death. *J Hepatol* **46**, 387–394.

Li, S., Tang, X., Seetharaman, J., Yang, C., Gu, Y., Zhang, J., Du, H., Shih, J. W., Hew, C. L. & other authors (2009). Dimerization of hepatitis E virus capsid protein E2s domain is essential for virus-host interaction. *PLoS Pathog* **5**, e1000537.

Magden, J., Takeda, N., Li, T., Auvinen, P., Ahola, T., Miyamura, T., Merits, A. & Kääriäinen, L. (2001). Virus-specific mRNA capping enzyme encoded by hepatitis E virus. *J Virol* **75**, 6249–6255.

Moin, S. M., Panteva, M. & Jameel, S. (2007). The hepatitis E virus Orf3 protein protects cells from mitochondrial depolarization and death. *J Biol Chem* **282**, 21124–21133.

Moin, S. M., Chandra, V., Arya, R. & Jameel, S. (2009). The hepatitis E virus ORF3 protein stabilizes HIF-1α and enhances HIF-1-mediated transcriptional activity through p300/CBP. *Cell Microbiol* **11**, 1409–1421.

Nanda, S. K., Panda, S. K., Durgapal, H. & Jameel, S. (1994). Detection of the negative strand of hepatitis E virus RNA in the livers of experimentally infected rhesus monkeys: evidence for viral replication. *J Med Virol* **42**, 237–240.

Panda, S. K., Nanda, S. K., Zafrullah, M., Ansari, I. H., Ozdener, M. H. & Jameel, S. (1995). An Indian strain of hepatitis E virus (HEV): cloning, sequence, and expression of structural region and antibody responses in sera from individuals from an area of high-level HEV endemicity. *J Clin Microbiol* **33**, 2653–2659.

Panda, S. K., Ansari, I. H., Durgapal, H., Agrawal, S. & Jameel, S. (2000). The in vitro-synthesized RNA from a cDNA clone of hepatitis E virus is infectious. *J Virol* **74**, 2430–2437.

Purdy, M., Tam, A., Huang, C., Yarbough, P. & Reyes, G. (1993). Hepatitis E virus: a non-enveloped member of the 'alpha-like' RNA virus supergroup. *Semin Virol* **4**, 319–326.

Rehman, S., Kapur, N., Durgapal, H. & Panda, S. K. (2008). Subcellular localization of hepatitis E virus (HEV) replicase. *Virology* **370**, 77–92.

Reyes, G. R., Purdy, M. A., Kim, J. P., Luk, K. C., Young, L. M., Fry, K. E. & Bradley, D. W. (1990). Isolation of a cDNA from the virus responsible for enterically transmitted non-A, non-B hepatitis. *Science* **247**, 1335–1339.

Reyes, G. R., Huang, C. C., Tam, A. W. & Purdy, M. A. (1993). Molecular organization and replication of hepatitis E virus (HEV). *Arch Virol Suppl* **7**, 15–25.

Sawicki, D. L. & Sawicki, S. G. (1980). Short-lived minus-strand polymerase for Semliki Forest virus. *J Virol* **34**, 108–118.

Sehgal, D., Thomas, S., Chakraborty, M. & Jameel, S. (2006). Expression and processing of the Hepatitis E virus ORF1 non-structural polyprotein. *Virol J* **3**, 38.

Strauss, J. H. & Strauss, E. G. (1994). The alphaviruses: gene expression, replication, and evolution. *Microbiol Rev* **58**, 491–562.

Takahashi, M., Yamada, K., Hoshino, Y., Takahashi, H., Ichiyama, K., Tanaka, T. & Okamoto, H. (2008). Monoclonal antibodies raised against the ORF3 protein of hepatitis E virus (HEV) can capture HEV particles in culture supernatant and serum but not those in feces. *Arch Virol* **153**, 1703–1713.

Tam, A. W., Smith, M. M., Guerra, M. E., Huang, C. C., Bradley, D. W., Fry, K. E. & Reyes, G. R. (1991). Hepatitis E virus (HEV): molecular cloning and sequencing of the full-length viral genome. *Virology* **185**, 120–131.

Tanaka, T., Takahashi, M., Kusano, E. & Okamoto, H. (2007). Development and evaluation of an efficient cell-culture system for hepatitis E virus. *J Gen Virol* **88**, 903–911.

Thakral, D., Nayak, B., Rehman, S., Durgapal, H. & Panda, S. K. (2005). Replication of a recombinant hepatitis E virus genome tagged with reporter genes and generation of a short-term cell line producing viral RNA and proteins. *J Gen Virol* **86**, 1189–1200.

Vishwanathan, R. (1957). Infectious hepatitis in Delhi (1955–56). A critical study: epidemiology. *Indian J Med Res* **45**, 49–58.

Wong, D. C., Purcell, R. H., Sreenivasan, M. A., Prasad, S. R. & Pavri, K. M. (1980). Epidemic and endemic hepatitis in India: evidence for a non-A, non-B hepatitis virus aetiology. *Lancet* **2**, 876–879.

Xia, X., Huang, R. & Li, D. (2000). Studies on the subgenomic RNAs of hepatitis E virus. *Wei Sheng Wu Xue Bao* **40**, 622–627 (in Chinese).

Yamada, K., Takahashi, M., Hoshino, Y., Takahashi, H., Ichiyama, K., Nagashima, S., Tanaka, T. & Okamoto, H. (2009). ORF3 protein of hepatitis E virus is essential for virion release from infected cells. *J Gen Virol* **90**, 1880–1891.

Yamashita, T., Mori, Y., Miyazaki, N., Cheng, R. H., Yoshimura, M., Unno, H., Shima, R., Moriishi, K., Tsukihara, T. & other authors (2009). Biological and immunological characteristics of hepatitis E virus-like particles based on the crystal structure. *Proc Natl Acad Sci U S A* **106**, 12986–12991.

Zafrullah, M., Ozdener, M. H., Panda, S. K. & Jameel, S. (1997). The ORF3 protein of hepatitis E virus is a phosphoprotein that associates with the cytoskeleton. *J Virol* **71**, 9045–9053.

Zhang, G. S., Feng, F. M., Li, Y. L., Yuan, J. X. & Shang, H. (2006). A study of chronic hepatitis B infection superinfected with hepatitis E infection. *Zhonghua Gan Zang Bing Za Zhi* **14**, 906–908 (in Chinese).